

Frank-Wolfe Optimization for Dominant Set Clustering

Carl Johnell, Morteza Haghir Chehreghani

Chalmers University of Technology
cjohnell@gmail.com, morteza.chehreghani@chalmers.se

Abstract

We study Frank-Wolfe algorithms – standard, pairwise, and away-steps – for efficient optimization of Dominant Set Clustering. We present a unified and computationally efficient framework to employ the different variants of Frank-Wolfe methods, and we investigate its effectiveness via several experimental studies. In addition, we provide explicit convergence rates for the algorithms in terms of the so called Frank-Wolfe gap. The theoretical analysis has been specialized to the problem of Dominant Set Clustering and is thus more easily accessible compared to prior work.

Introduction

Data clustering plays an important role in unsupervised learning and exploratory data analytics (Jain 2010). It is used in many applications and areas such as network analysis, image segmentation, document and text processing, community detection and bioinformatics. Given a set of n objects with indices $V = \{1, \dots, n\}$ and the nonnegative pairwise similarities $\mathbf{A} = (a_{ij})$, i.e., graph $\mathcal{G}(V, \mathbf{A})$ with vertices V and edge weights \mathbf{A} , our goal is to partition the data into coherent groups that look dissimilar from each other. We assume zero self-similarities, i.e., $a_{ii} = 0 \forall i$. Several clustering methods compute the clusters via minimizing a cost function. Examples are Ratio Cut (Chan, Schlag, and Zien 1994), Normalized Cut (Shi and Malik 2000), Correlation Clustering (Bansal, Blum, and Chawla 2004), and shifted Min Cut (Haghir Chehreghani 2017a). For some of them, for example Normalized Cut, approximate solutions have been developed in the context of spectral analysis (Shi and Malik 2000; Ng, Jordan, and Weiss 2001), Power Iteration method (Lin and Cohen 2010) and P-Spectral Clustering (Bühler and Hein 2009; Hein and Bühler 2010). It is notable that clustering can be applied to more complicated data such as trees (Haghir Chehreghani et al. 2007).

Another prominent clustering approach has been developed in the context of Dominant Set Clustering (DSC) and its connection to discrete-time dynamical systems and *replicator dynamics* (Pavan and Pelillo 2007; Bulò and Pelillo 2017). Unlike the methods based on cost function minimization, DSC does not define a global cost function for the clusters. Instead, it applies the generic principles of clustering where each cluster should be coherent and well separated from the other clusters. These principles are formu-

lated via the concepts of dominant sets (Pavan and Pelillo 2007). Then, several variants of the method have been proposed. The method in (Liu, Latecki, and Yan 2013) proposes an iterative clustering algorithm in two Shrink and Expand steps. These steps are suitable for sparse data and lead to reducing the runtime of performing replicator dynamics. (Bulò, Torsello, and Pelillo 2009) develops an enumeration technique for different clusters via unstabilizing the underlying equilibrium of replicator dynamics. (Pavan and Pelillo 2003a) proposes a hierarchical variant of DSC via regularization and shifting the off-diagonal elements of the similarity matrix. (Chehreghani 2016) analyzes adaptively the trajectories of replicator dynamics in order to discover suitable phase transitions that correspond to different clusters. Several studies demonstrate the effectiveness of DSC variants compared to other clustering methods, such as spectral methods (Pavan and Pelillo 2007; Liu, Latecki, and Yan 2013; Chehreghani 2016; Bulò and Pelillo 2017).

In this paper, we investigate efficient optimization for DSC based on Frank-Wolfe algorithms (Frank and Wolfe 1956; Lacoste-Julien and Jaggi 2015; Reddi et al. 2016) instead of replicator dynamics. Frank-Wolfe optimization has been successfully applied to several constrained optimization problems. We develop a unified and computationally efficient framework to employ the different variants of Frank-Wolfe algorithms for DSC, and we investigate its effectiveness via several experimental studies. Our theoretical analysis is specialized to DSC, and we provide explicit convergence rates for the algorithms in terms of the so called Frank-Wolfe gap – including pairwise Frank-Wolfe with nonconvex/nonconcave objective function, which we have not seen in prior work.

Dominant Set Clustering

DSC follows an iterative procedure to compute the clusters: i) compute a dominant set using the similarity matrix \mathbf{A} of the available data, ii) peel off (remove) the clustered objects from the data, and iii) repeat until a predefined number of clusters have been obtained.¹

¹With some abuse of the notation, n , V , \mathbf{A} and \mathbf{x} sometimes refer to the available (i.e., still unclustered) objects and the similarities between them. This is obvious from the context.

Dominant sets correspond to local optima of the following quadratic problem (Pavan and Pelillo 2007), called standard quadratic problem (StQP).

$$\begin{aligned} & \text{maximize } f(\mathbf{x}) = \mathbf{x}^T \mathbf{A} \mathbf{x} \\ & \text{subject to } \mathbf{x} \in \Delta = \left\{ \mathbf{x} \in \mathbb{R}^n : \mathbf{x} \geq \mathbf{0}^n \text{ and } \sum_{i=1}^n x_i = 1 \right\}. \end{aligned} \quad (1)$$

The constraint Δ is called the standard simplex. We note that \mathbf{A} is generally not negative definite, and the objective function $f(\mathbf{x})$ is thus *not* concave.

Every unclustered object i corresponds to a component of the n -dimensional characteristic vector \mathbf{x} . The support of local optimum \mathbf{x}^* specifies the objects that belong to the dominant set (cluster), i.e., i is in the cluster if component $x_i^* > 0$. In practice we use $x_i^* > \delta$, where δ is a small number called the cutoff parameter. Previous work employ replicator dynamics to solve StQP, where \mathbf{x} is updated according to the following dynamics.

$$x_i^{(t+1)} = x_i^{(t)} \frac{(\mathbf{A} \mathbf{x}_t)_i}{\mathbf{x}_t^T \mathbf{A} \mathbf{x}_t}, i = 1, \dots, n, \quad (2)$$

where \mathbf{x}_t indicates the solution at iterate t , and $x_i^{(t)}$ is the i -th component of \mathbf{x}_t . Note the $\mathcal{O}(n^2)$ per-iteration time complexity due to the matrix multiplication.

In this paper we investigate an alternative optimization framework based on Frank-Wolfe methods.

Unified Frank-Wolfe Optimization Methods

Let $\mathcal{P} \subset \mathbb{R}^n$ be a finite set of points and $\mathcal{D} = \text{convex}(\mathcal{P})$ its convex hull (convex polytope). The Frank-Wolfe algorithm, first introduced in (Frank and Wolfe 1956), aims at solving the following constrained optimization.

$$\max_{\mathbf{x} \in \mathcal{D}} f(\mathbf{x}), \quad (3)$$

where f is nonlinear and differentiable. The formulation in (Lacoste-Julien 2016) has extended the concavity assumption to arbitrary functions with L -Lipschitz ('well-behaved') gradients. Algorithm 1 outlines the steps of a Frank-Wolfe method to solve the optimization in (3).

Algorithm 1 Frank-Wolfe pseudocode

```

1: procedure PSEUDO-FW( $f, \mathcal{D}, T$ )    ▷ Function  $f$ ,
   convex polytope  $\mathcal{D}$ , and iterations  $T$ .
2:   Select  $\mathbf{x}_0 \in \mathcal{D}$ 
3:   for  $t = 0, \dots, T - 1$  do
4:     if  $\mathbf{x}_t$  is stationary then break
5:     Compute feasible ascent direction  $\mathbf{d}_t$  at  $\mathbf{x}_t$ 
6:     Compute step size  $\gamma_t \in [0, 1]$  such that  $f(\mathbf{x}_t + \gamma_t \mathbf{d}_t) > f(\mathbf{x}_t)$ 
7:      $\mathbf{x}_{t+1} := \mathbf{x}_t + \gamma_t \mathbf{d}_t$ 
8:   return  $\mathbf{x}_t$ 

```

In this work, in addition to the standard FW (called FW), we also consider two other variants of FW: pairwise FW

(PFW) and away-steps FW (AFW), adapted from (Lacoste-Julien and Jaggi 2015). They differ in the way the ascent direction \mathbf{d}_t is computed.

From the definition of \mathcal{D} , any point $\mathbf{x}_t \in \mathcal{D}$ can be written as a convex combination of the points in \mathcal{P} , i.e.,

$$\mathbf{x}_t = \sum_{\mathbf{v} \in \mathcal{P}} \lambda_{\mathbf{v}}^{(t)} \mathbf{v}, \quad (4)$$

where the coefficients $\lambda_{\mathbf{v}}^{(t)} \in [0, 1]$ and $\sum_{\mathbf{v} \in \mathcal{P}} \lambda_{\mathbf{v}}^{(t)} = 1$. Define

$$S_t = \{\mathbf{v} \in \mathcal{P} : \lambda_{\mathbf{v}}^{(t)} > 0\} \quad (5)$$

as the set of points with nonzero coefficients at iterate t . Moreover, let

$$\mathbf{s}_t \in \arg \max_{\mathbf{s} \in \mathcal{D}} \nabla f(\mathbf{x}_t)^T \mathbf{s}, \quad (6)$$

$$\mathbf{v}_t \in \arg \min_{\mathbf{v} \in S_t} \nabla f(\mathbf{x}_t)^T \mathbf{v}. \quad (7)$$

Since \mathcal{D} is a convex polytope, \mathbf{s}_t is the point that maximizes the linearization and \mathbf{v}_t is the point with nonzero coefficient that minimizes it over S_t . Let \mathbf{x}_t be the estimated solution of (3) at iterate t and define

$$\begin{aligned} \mathbf{d}_t^A &= \mathbf{x}_t - \mathbf{v}_t, \\ \mathbf{d}_t^{FW} &= \mathbf{s}_t - \mathbf{x}_t, \\ \mathbf{d}_t^{AFW} &= \begin{cases} \mathbf{d}_t^{FW}, & \text{if } \nabla f(\mathbf{x}_t)^T \mathbf{d}_t^{FW} \geq f(\mathbf{x}_t)^T \mathbf{d}_t^A \\ \frac{\lambda_{\mathbf{v}_t}^{(t)}}{1 - \lambda_{\mathbf{v}_t}^{(t)}} \mathbf{d}_t^A, & \text{otherwise} \end{cases} \\ \mathbf{d}_t^{PFW} &= \mathbf{s}_t - \mathbf{v}_t \end{aligned} \quad (8)$$

respectively as the away, FW, pairwise, and away/FW directions. The FW direction moves towards a 'good' point, and the away direction moves away from a 'bad' point. The pairwise direction shifts from a 'bad' point to a 'good' point (Lacoste-Julien and Jaggi 2015). The coefficient with \mathbf{d}_t^A in \mathbf{d}_t^{AFW} ensures the next iterate remains feasible.

An issue with standard FW, which PFW and AFW aim to fix, is the zig-zagging phenomenon. This occurs when the optimal solution of (3) lies on the boundary of the domain. Then the iterates start to *zig-zag* between the points, which negatively affects the convergence. By adding the possibility of an away step in AFW, or alternatively using the pairwise direction, the zig-zagging can be attenuated.

The step size γ_t can be computed by line-search, i.e.,

$$\gamma_t \in \arg \max_{\gamma \in [0, 1]} f(\mathbf{x}_t + \gamma \mathbf{d}_t). \quad (9)$$

Finally, the Frank-Wolfe gap is used to check if an iterate is (close enough to) a stationary solution.

Definition 1. The Frank-Wolfe gap g_t of $f : \mathcal{D} \rightarrow \mathbb{R}$ at iterate \mathbf{x}_t is defined as

$$\begin{aligned} g_t &= \max_{\mathbf{s} \in \mathcal{D}} \nabla f(\mathbf{x}_t)^T (\mathbf{s} - \mathbf{x}_t) \\ &\iff \\ g_t &= \nabla f(\mathbf{x}_t)^T \mathbf{d}_t^{FW}. \end{aligned} \quad (10)$$

A point \mathbf{x}_t is stationary if and only if $g_t = 0$, meaning there are no ascent directions. The Frank-Wolfe gap is thus a reasonable measure of nonstationarity and is frequently used as a stopping criterion (Lacoste-Julien 2016). Specifically, a threshold ϵ is defined, and if $g_t \leq \epsilon$, then we conclude the iterate is sufficiently close to a stationary point and stop the algorithm.

Frank-Wolfe for Dominant Set Clustering

Here we apply the Frank-Wolfe methods from the previous section to the optimization problem (1) defined by DSC.

Simplex Domain Because of the simplex form – the constraints in (1) – the convex combination in (4) for $\mathbf{x} \in \Delta$ can be written as

$$\mathbf{x} = \sum_{i=1}^n \lambda_{\mathbf{e}_i} \mathbf{e}_i, \quad (11)$$

where \mathbf{e}_i are the standard basis vectors. That is, the i -th coefficient corresponds to the i -th component of \mathbf{x} , $\lambda_{\mathbf{e}_i} = x_i$. The set of components with nonzero coefficients at iterate \mathbf{x}_t gives the support, i.e.,

$$\sigma_t = \{i \in V : x_i^{(t)} > 0\}. \quad (12)$$

Due to the structure of the simplex Δ , the solution of the optimization (6) is

$$\begin{cases} \mathbf{s}_t & \in \Delta \\ s_i^{(t)} & = 1, \quad \text{where } i \in \arg \max_i \nabla_i f(\mathbf{x}_t) \\ s_j^{(t)} & = 0, \quad \text{for } j \neq i, \end{cases} \quad (13)$$

and the optimization (7) is obtained by

$$\begin{cases} \mathbf{v}_t & \in \Delta \\ v_i^{(t)} & = 1, \quad \text{where } i \in \arg \min_{i \in \sigma_t} \nabla_i f(\mathbf{x}_t) \\ v_j^{(t)} & = 0, \quad \text{for } j \neq i. \end{cases} \quad (14)$$

The maximum and minimum values of the linearization are the largest and smallest components of the gradient, respectively (subject to $i \in \sigma_t$ in the latter case). Note that the gradient is $\nabla f(\mathbf{x}_t) = 2\mathbf{A}\mathbf{x}_t$.

Step Sizes We compute the optimal step sizes for FW, PFW, and AFW. Iterate subscripts t are omitted for clarity. We define the step size function as

$$\begin{aligned} \psi(\gamma) &= f(\mathbf{x} + \gamma \mathbf{d}) \\ &= (\mathbf{x} + \gamma \mathbf{d})^T \mathbf{A}(\mathbf{x} + \gamma \mathbf{d}) \\ &= \mathbf{x}^T \mathbf{A} \mathbf{x} + 2\gamma \mathbf{d}^T \mathbf{A} \mathbf{x} + \gamma^2 \mathbf{d}^T \mathbf{A} \mathbf{d} \\ &= f(\mathbf{x}) + \gamma \nabla f(\mathbf{x}_t)^T \mathbf{d} + \gamma^2 \mathbf{d}^T \mathbf{A} \mathbf{d}, \end{aligned} \quad (15)$$

for some ascent direction \mathbf{d} . This expression is a single variable second degree polynomial in γ . The function is concave if the coefficient $\mathbf{d}^T \mathbf{A} \mathbf{d} \leq 0$ – second derivative test – and admits a global maximum in that case.

In the following it is assumed that \mathbf{s} and \mathbf{v} satisfy (13) and (14), and their nonzero components are i and j , respectively.

FW direction: Substitute $\mathbf{d}^{FW} = \mathbf{s} - \mathbf{x}$ into $\mathbf{d}^T \mathbf{A} \mathbf{d}$.

$$\begin{aligned} \mathbf{d}^T \mathbf{A} \mathbf{d} &= (\mathbf{s} - \mathbf{x})^T \mathbf{A}(\mathbf{s} - \mathbf{x}) \\ &= \mathbf{s}^T \mathbf{A} \mathbf{s} - 2\mathbf{s}^T \mathbf{A} \mathbf{x} + \mathbf{x}^T \mathbf{A} \mathbf{x} \\ &= -(2\mathbf{s}^T \mathbf{A} \mathbf{x} - \mathbf{x}^T \mathbf{A} \mathbf{x}) \\ &= \mathbf{x}^T \mathbf{A} \mathbf{x} - 2\mathbf{a}_{i*}^T \mathbf{x}. \end{aligned} \quad (16)$$

The i -th row of \mathbf{A} is \mathbf{a}_{i*} and the j -th column of \mathbf{A} is \mathbf{a}_{*j} .

Pairwise direction: Substitute $\mathbf{d}^{PFW} = \mathbf{s} - \mathbf{v}$ into $\mathbf{d}^T \mathbf{A} \mathbf{d}$.

$$\begin{aligned} \mathbf{d}^T \mathbf{A} \mathbf{d} &= (\mathbf{s} - \mathbf{v})^T \mathbf{A}(\mathbf{s} - \mathbf{v}) \\ &= \mathbf{s}^T \mathbf{A} \mathbf{s} - 2\mathbf{v}^T \mathbf{A} \mathbf{s} + \mathbf{v}^T \mathbf{A} \mathbf{v} \\ &= -2a_{ij}. \end{aligned} \quad (17)$$

Away direction: Substitute $\mathbf{d}^A = \mathbf{x} - \mathbf{v}$ into $\mathbf{d}^T \mathbf{A} \mathbf{d}$.

$$\begin{aligned} \mathbf{d}^T \mathbf{A} \mathbf{d} &= (\mathbf{x} - \mathbf{v})^T \mathbf{A}(\mathbf{x} - \mathbf{v}) \\ &= \mathbf{x}^T \mathbf{A} \mathbf{x} - 2\mathbf{v}^T \mathbf{A} \mathbf{x} + \mathbf{v}^T \mathbf{A} \mathbf{v} \\ &= \mathbf{x}^T \mathbf{A} \mathbf{x} - 2\mathbf{a}_{j*}^T \mathbf{x}. \end{aligned} \quad (18)$$

Recall \mathbf{A} has nonnegative entries and zeros on the main diagonal. Therefore $\mathbf{s}^T \mathbf{A} \mathbf{s} = 0$ and $\mathbf{v}^T \mathbf{A} \mathbf{v} = 0$. It is immediate that (17) is nonpositive. From $\mathbf{x}^T \mathbf{A} \mathbf{x} \leq \mathbf{s}^T \mathbf{A} \mathbf{x}$ we conclude that (16) is also nonpositive. The corresponding step size functions are therefore always *concave*. We cannot make any conclusion for (18), and the sign of $\mathbf{d}^T \mathbf{A} \mathbf{d}$ is therefore dependent on the iterate.

The derivative of $\psi(\gamma)$ is

$$\frac{d\psi}{d\gamma}(\gamma) = \nabla f(\mathbf{x})^T \mathbf{d} + 2\gamma \mathbf{d}^T \mathbf{A} \mathbf{d}. \quad (19)$$

By solving $\frac{d\psi}{d\gamma}(\gamma) = 0$ we obtain

$$\begin{aligned} \nabla f(\mathbf{x})^T \mathbf{d} + 2\gamma \mathbf{d}^T \mathbf{A} \mathbf{d} &= 0 \\ \iff \\ \gamma^* &= -\frac{\nabla f(\mathbf{x})^T \mathbf{d}}{2\mathbf{d}^T \mathbf{A} \mathbf{d}} = -\frac{\mathbf{x}^T \mathbf{A} \mathbf{d}}{\mathbf{d}^T \mathbf{A} \mathbf{d}}. \end{aligned} \quad (20)$$

Since $\nabla f(\mathbf{x})^T \mathbf{d} \geq 0$, we also conclude here that $\mathbf{d}^T \mathbf{A} \mathbf{d} < 0$ has to hold in order for the step size to make sense.

By substituting the directions and corresponding $\mathbf{d}^T \mathbf{A} \mathbf{d}$ into (20) we obtain the different step sizes.

FW direction and (16):

$$\gamma^{FW} = -\frac{\mathbf{x}^T \mathbf{A} \mathbf{d}}{\mathbf{d}^T \mathbf{A} \mathbf{d}} = \frac{\mathbf{a}_{i*}^T \mathbf{x} - \mathbf{x}^T \mathbf{A} \mathbf{x}}{2\mathbf{a}_{i*}^T \mathbf{x} - \mathbf{x}^T \mathbf{A} \mathbf{x}}. \quad (21)$$

Pairwise direction and (17):

$$\gamma^{PFW} = -\frac{\mathbf{x}^T \mathbf{A} \mathbf{d}}{\mathbf{d}^T \mathbf{A} \mathbf{d}} = \frac{\mathbf{a}_{i*}^T \mathbf{x} - \mathbf{a}_{j*}^T \mathbf{x}}{2a_{ij}}. \quad (22)$$

Away direction and (18):

$$\gamma^A = -\frac{\mathbf{x}^T \mathbf{A} \mathbf{d}}{\mathbf{d}^T \mathbf{A} \mathbf{d}} = \frac{\mathbf{x}^T \mathbf{A} \mathbf{x} - \mathbf{a}_{j*}^T \mathbf{x}}{2\mathbf{a}_{j*}^T \mathbf{x} - \mathbf{x}^T \mathbf{A} \mathbf{x}}. \quad (23)$$

Algorithms Here, we describe in detail standard FW (Algorithm 2), pairwise FW (Algorithm 3), and away-steps FW (Algorithm 4) for problem (1), following the high-level structure of Algorithm 1. All variants have $\mathcal{O}(n)$ per-iteration time complexity, where the linear operations are $\arg \max$, $\arg \min$, and vector addition. The key for this time complexity is that we are able to update the gradient $\nabla f(\mathbf{x}) = 2\mathbf{A}\mathbf{x}$ in linear time. Lemmas 1, 2, and 3 show why this is the case. Recall that the updates in replicator dynamics are quadratic w.r.t. n .

Algorithm 2 FW for DSC

```

1: procedure FW( $\mathbf{A}, \epsilon, T$ )
2:   Select  $\mathbf{x}_0 \in \Delta$ 
3:    $\mathbf{r}_0 := \mathbf{A}\mathbf{x}_0$ 
4:    $f_0 := \mathbf{r}_0^T \mathbf{x}_0$ 
5:   for  $t = 0, \dots, T - 1$  do
6:      $\mathbf{s}_t := \mathbf{e}_i$ , where  $i \in \arg \max_{\ell} r_{\ell}^{(t)}$ 
7:      $g_t := r_i^{(t)} - f_t$ 
8:     if  $g_t \leq \epsilon$  then break
9:      $\gamma_t := \frac{r_i^{(t)} - f_t}{2r_i^{(t)} - f_t}$ 
10:     $\mathbf{x}_{t+1} := (1 - \gamma_t)\mathbf{x}_t + \gamma_t \mathbf{s}_t$ 
11:     $\mathbf{r}_{t+1} := (1 - \gamma_t)\mathbf{r}_t + \gamma_t \mathbf{a}_{*i}$ 
12:     $f_{t+1} := (1 - \gamma_t)^2 f_t + 2\gamma_t(1 - \gamma_t)r_i^{(t)}$ 
13:  return  $\mathbf{x}_t$ 

```

Lemma 1. For $\mathbf{x}_{t+1} = (1 - \gamma_t)\mathbf{x}_t + \gamma_t \mathbf{s}_t$, lines 11 and 12 in Algorithm 2 satisfy

$$\begin{aligned} \mathbf{r}_{t+1} &= \mathbf{A}\mathbf{x}_{t+1}, \\ f_{t+1} &= \mathbf{x}_{t+1}^T \mathbf{A}\mathbf{x}_{t+1}. \end{aligned}$$

Algorithm 3 Pairwise FW for DSC

```

1: procedure PFW( $\mathbf{A}, \epsilon, T$ )
2:   Select  $\mathbf{x}_0 \in \Delta$ 
3:    $\mathbf{r}_0 := \mathbf{A}\mathbf{x}_0$ 
4:    $f_0 := \mathbf{r}_0^T \mathbf{x}_0$ 
5:   for  $t = 0, \dots, T - 1$  do
6:      $\sigma_t := \{i \in V : x_i^{(t)} > 0\}$ 
7:      $\mathbf{s}_t := \mathbf{e}_i$ , where  $i \in \arg \max_{\ell} r_{\ell}^{(t)}$ 
8:      $\mathbf{v}_t := \mathbf{e}_j$ , where  $j \in \arg \min_{\ell \in \sigma_t} r_{\ell}^{(t)}$ 
9:      $g_t := r_i^{(t)} - f_t$ 
10:    if  $g_t \leq \epsilon$  then break
11:     $\gamma_t := \min \left( x_j^{(t)}, \frac{r_i^{(t)} - r_j^{(t)}}{2a_{ij}} \right)$ 
12:     $\mathbf{x}_{t+1} := \mathbf{x}_t + \gamma_t(\mathbf{s}_t - \mathbf{v}_t)$ 
13:     $\mathbf{r}_{t+1} := \mathbf{r}_t + \gamma_t(\mathbf{a}_{*i} - \mathbf{a}_{*j})$ 
14:     $f_{t+1} := f_t + 2\gamma_t(r_i^{(t)} - r_j^{(t)}) - 2\gamma_t^2 a_{ij}$ 
15:  return  $\mathbf{x}_t$ 

```

Lemma 2. For $\mathbf{x}_{t+1} = \mathbf{x}_t + \gamma_t(\mathbf{s}_t - \mathbf{v}_t)$, lines 13 and 14 in Algorithm 3 satisfy

$$\begin{aligned} \mathbf{r}_{t+1} &= \mathbf{A}\mathbf{x}_{t+1}, \\ f_{t+1} &= \mathbf{x}_{t+1}^T \mathbf{A}\mathbf{x}_{t+1}. \end{aligned}$$

Algorithm 4 Away-steps FW for DSC

```

1: procedure AFW( $\mathbf{A}, \epsilon, T$ )
2:   Select  $\mathbf{x}_0 \in \Delta$ 
3:    $\mathbf{r}_0 := \mathbf{A}\mathbf{x}_0$ 
4:    $f_0 := \mathbf{r}_0^T \mathbf{x}_0$ 
5:   for  $t = 0, \dots, T - 1$  do
6:      $\sigma_t := \{i \in V : x_i^{(t)} > 0\}$ 
7:      $\mathbf{s}_t := \mathbf{e}_i$ , where  $i \in \arg \max_{\ell} r_{\ell}^{(t)}$ 
8:      $\mathbf{v}_t := \mathbf{e}_j$ , where  $j \in \arg \min_{\ell \in \sigma_t} r_{\ell}^{(t)}$ 
9:      $g_t := r_i^{(t)} - f_t$ 
10:    if  $g_t \leq \epsilon$  then break
11:    if  $(r_i^{(t)} - f_t) \geq (f_t - r_j^{(t)})$  then  $\triangleright$  FW direction
12:       $\gamma_t := \frac{r_i^{(t)} - f_t}{2r_i^{(t)} - f_t}$ 
13:       $\mathbf{x}_{t+1} := (1 - \gamma_t)\mathbf{x}_t + \gamma_t \mathbf{s}_t$ 
14:       $\mathbf{r}_{t+1} := (1 - \gamma_t)\mathbf{r}_t + \gamma_t \mathbf{a}_{*i}$ 
15:       $f_{t+1} := (1 - \gamma_t)^2 f_t + 2\gamma_t(1 - \gamma_t)r_i^{(t)}$ 
16:    else  $\triangleright$  Away direction
17:       $\gamma_t := x_j^{(t)} / (1 - x_j^{(t)})$ 
18:      if  $(2r_j^{(t)} - f_t) > 0$  then
19:         $\gamma_t \leftarrow \min \left( \gamma_t, \frac{f_t - r_j^{(t)}}{2r_j^{(t)} - f_t} \right)$ 
20:       $\mathbf{x}_{t+1} := (1 + \gamma_t)\mathbf{x}_t - \gamma_t \mathbf{v}_t$ 
21:       $\mathbf{r}_{t+1} := (1 + \gamma_t)\mathbf{r}_t - \gamma_t \mathbf{a}_{*j}$ 
22:       $f_{t+1} := (1 + \gamma_t)^2 f_t - 2\gamma_t(1 + \gamma_t)r_j^{(t)}$ 
23:  return  $\mathbf{x}_t$ 

```

Lines 12-15 are identical to the updates in Algorithm 2 and are included in Lemma 1. We therefore only show the away direction.

Lemma 3. For $\mathbf{x}_{t+1} = (1 + \gamma_t)\mathbf{x}_t - \gamma_t \mathbf{v}_t$, lines 22 and 23 in Algorithm 4 satisfy

$$\begin{aligned} \mathbf{r}_{t+1} &= \mathbf{A}\mathbf{x}_{t+1}, \\ f_{t+1} &= \mathbf{x}_{t+1}^T \mathbf{A}\mathbf{x}_{t+1}. \end{aligned}$$

Algorithm 4 (AFW) is actually equivalent to the infection and immunization dynamics (InImDyn) with the pure strategy selection function, introduced in (Bulò, Pelillo, and Bomze 2011) as an alternative to replicator dynamics. However, InImDyn is derived from the perspective of evolutionary game theory as opposed to Frank-Wolfe. Thus, our framework provides a different way to analyze this method and also study its convergence rate.

Proposition 4. Algorithm 4 (AFW) is equivalent to Algorithm 1 in (Bulò, Pelillo, and Bomze 2011).

Analysis of Convergence Rates

(Lacoste-Julien 2016) shows that the Frank-Wolfe gap for standard FW decreases at rate $\mathcal{O}(1/\sqrt{t})$ for nonconvex/nonconcave objective functions, where t is the number of iterations. A similar convergence rate is shown in (Bomze, Rinaldi, and Zeffiro 2019) for nonconvex AFW over the simplex. When the objective function is convex/concave, linear convergence rates for PFW and AFW are shown in (Lacoste-Julien and Jaggi 2015). The analysis in (Thiel, Haghir Chehreghani, and Dubhashi 2019) shows linear convergence rate of standard FW for nonconvex but multi-linear functions. We are not aware of any work analyzing the convergence rate in terms of the Frank-Wolfe gap for nonconvex/nonconcave PFW.

Following the terminology and techniques in (Lacoste-Julien 2016; Lacoste-Julien and Jaggi 2015; Bomze, Rinaldi, and Zeffiro 2019), we present a unified framework to analyze convergence rates for Algorithms 2, 3, and 4. The analysis is split into a number of different cases, where each case handles a unique ascent direction and step size combination. For the step sizes, we consider one case when the optimal step size is used ($\gamma_t < \gamma_{max}$), and a second case when it has been truncated ($\gamma_t = \gamma_{max}$). The former case is referred to as a good step, since in this case we can provide a lower bound on the progress $f(\mathbf{x}_{t+1}) - f(\mathbf{x}_t)$ in terms of the Frank-Wolfe gap. The latter case is referred to as a drop step or a swap step. It is called a drop step when the cardinality of the support reduces by one, i.e., $|\sigma_{t+1}| = |\sigma_t| - 1$, and it is called a swap step when it remains unchanged, i.e., $|\sigma_{t+1}| = |\sigma_t|$. When $\gamma_t = \gamma_{max}$ we cannot provide a bound on the progress in terms of the Frank-Wolfe gap, and instead we bound the number of drop/swap steps. Furthermore, this case can only happen for PFW and AFW as the step size for FW always satisfies $\gamma_t < \gamma_{max}$. Swap steps can only happen for PFW.

Let

$$\tilde{g}_t = \min_{0 \leq \ell \leq t} g_\ell, \quad \underline{M} = \min_{i,j:i \neq j} a_{ij}, \quad \overline{M} = \max_{i,j:i \neq j} a_{ij},$$

be the smallest Frank-Wolfe gap after t iterations, and the smallest and largest off-diagonal elements of \mathbf{A} . Let I be the indexes that take a good step. That is, for $t \in I$ we have $\gamma_t < \gamma_{max}$. Then, we show the following results (the details are in supplemental).

Lemma 5. *The smallest Frank-Wolfe gap for Algorithms 2, 3, and 4 satisfy*

$$\tilde{g}_t \leq 2\sqrt{\frac{\beta(f(\mathbf{x}_t) - f(\mathbf{x}_0))}{|I|}}, \quad (24)$$

where $\beta = 2\overline{M} - \underline{M}$ for FW and AFW, and $\beta = 2\overline{M}$ for PFW.

Theorem 6. *The smallest Frank-Wolfe gap for Algorithm 2 (FW) satisfies*

$$\tilde{g}_t^{FW} \leq 2\sqrt{\frac{(2\overline{M} - \underline{M})(f(\mathbf{x}_t) - f(\mathbf{x}_0))}{t}}. \quad (25)$$

Theorem 7. *The smallest Frank-Wolfe gap for Algorithm 3 (PFW) satisfies*

$$\tilde{g}_t^{PFW} \leq 2\sqrt{\frac{6n!\overline{M}(f(\mathbf{x}_t) - f(\mathbf{x}_0))}{t}}. \quad (26)$$

Theorem 8. *The smallest Frank-Wolfe gap for Algorithm 4 (AFW) satisfies*

$$\tilde{g}_t^{AFW} \leq 2\sqrt{\frac{2(2\overline{M} - \underline{M})(f(\mathbf{x}_t) - f(\mathbf{x}_0))}{t + 1 - |\sigma_0|}}. \quad (27)$$

From Theorems 6, 7 and 8 we conclude Corollary 9.

Corollary 9. *The smallest Frank-Wolfe gap for Algorithms 2, 3, and 4 decrease at rate $\mathcal{O}(1/\sqrt{t})$.*

Initialization

The way the algorithms are initialized – value of \mathbf{x}_0 – affects the local optima the algorithms converge to. Let $\bar{\mathbf{x}}^B = \frac{1}{n}\mathbf{e}$ be the barycenter of the simplex Δ , where $\mathbf{e}^T = (1, 1, \dots, 1)$. We also define $\bar{\mathbf{x}}^V$ as

$$\begin{cases} \bar{\mathbf{x}}^V \in \Delta \\ \bar{x}_i^V = 1, & \text{where } i \in \arg \max_i \nabla_i f(\bar{\mathbf{x}}^B) \\ \bar{x}_j^V = 0, & \text{for } j \neq i. \end{cases} \quad (28)$$

Initializing \mathbf{x}_0 with $\bar{\mathbf{x}}^B$ avoids initial bias to a particular solution as it considers a uniform distribution over the available objects. Since $\nabla f(\bar{\mathbf{x}}^B) = 2\mathbf{A}\bar{\mathbf{x}}^B$, the nonzero component of $\bar{\mathbf{x}}^V$ corresponds to the row of \mathbf{A} with largest total sum. Therefore, it is biased to an object that is highly similar to many other objects.

The starting point for replicator dynamics is $\bar{\mathbf{x}}^{RD} = \bar{\mathbf{x}}^B$, as used for example in (Pavan and Pelillo 2003b; Pavan and Pelillo 2007). Note that if a component of $\bar{\mathbf{x}}^{RD}$ starts at zero it will remain at zero for the entire duration of the dynamics according to (2). Furthermore, $(\bar{\mathbf{x}}^V)^T \mathbf{A} \bar{\mathbf{x}}^V = 0$ since \mathbf{A} has zeros on the main diagonal, and the denominator in replicator dynamics is then zero for this point. Thus, $\bar{\mathbf{x}}^V$ is not a viable starting point for replicator dynamics.

The starting point for standard FW is $\bar{\mathbf{x}}^{FW} = \bar{\mathbf{x}}^V$, and was found experimentally to work well. As explained in convergence rate analysis, FW never performs any drop steps since the step size always satisfies $\gamma_t < \gamma_{max}$. Hence, using $\bar{\mathbf{x}}^B$ as starting point for FW will lead to a solution that has full support – this was found experimentally to hold true as well. Therefore, with FW, we use only initialization with $\bar{\mathbf{x}}^V$. With PFW and AFW, we can use both $\bar{\mathbf{x}}^B$ and $\bar{\mathbf{x}}^V$ as starting points. We denote the PFW and AFW variants by PFW-B, PFW-V, AFW-B, and AFW-V, respectively, to specify the starting point.

Experiments

In this section, we describe the experimental results of the different optimization methods.

Experimental Setup

Settings. The Frank-Wolfe gap (Definition 1) and the distance between two consecutive iterates are used as the stopping criterion for the FW variants and replicator dynamics. Specifically, let ϵ be the threshold, then an algorithm stops if $g_t \leq \epsilon$ or if $\|\mathbf{x}_{t+1} - \mathbf{x}_t\| \leq \epsilon$. In the experiments we set ϵ to Python’s epsilon, $\epsilon \approx 2.2 \cdot 10^{-16}$, and the cutoff parameter δ to $\delta = 2 \cdot 10^{-12}$.

We denote the number of clusters in the dataset by k and the maximum number of clusters to extract by K . For a dataset with n objects, the clustering assignment is represented by a discrete n -dimensional vector \mathbf{c} , i.e., $c_i \in \{0, 1, \dots, K-1, K\}$ for $i = 1, \dots, n$. If $c_i = c_j$, then objects i and j are in the same cluster. The discrete values $0, 1, \dots, K-1, K$ are called labels and represent the different clusters. Label 0 is designated to represent ‘no cluster’ – if $c_i = 0$, then object i is unassigned. We may regularize the pairwise similarities by a shift parameter, as described in detail in (Johnell 2020).

Clustering metrics. To evaluate the clustering quality, we compare the predicted solution and the ground truth solution w.r.t. Adjusted Rand Index (ARI) (Hubert and Arabie 1985) and V-Measure (Rosenberg and Hirschberg 2007). The Rand index is the ratio of the object pairs that are either in the same cluster or in different clusters, in both the predicted and ground truth solutions. V-measure is the harmonic mean of homogeneity and completeness. We may also report the Assignment Rate (AR), representing the rate of the objects assigned to a valid cluster.

	t	time	AR	ARI	V-Meas.
FW	1000	0.36s	0.6325	0.4695	0.5388
	4000	1.35s	0.6885	0.4593	0.5224
	8000	2.41s	0.6969	0.4673	0.5325
PFW-B	1000	0.43s	0.7429	0.1944	0.4289
	4000	1.86s	0.6605	0.467	0.5327
	8000	2.62s	0.642	0.471	0.5335
PFW-V	1000	0.52s	0.6471	0.5178	0.5745
	4000	1.6s	0.6487	0.4565	0.5237
	8000	2.47s	0.642	0.471	0.5335
AFW-B	1000	0.35s	0.8527	0.076	0.2854
	4000	1.69s	0.6258	0.3887	0.5316
	8000	2.93s	0.6599	0.4676	0.5328
AFW-V	1000	0.46s	0.6415	0.5184	0.5736
	4000	1.38s	0.6482	0.518	0.5754
	8000	2.75s	0.6476	0.4618	0.5257
RD	1000	1.06s	1.0	0.0	0.0
	4000	4.56s	0.9081	0.1852	0.3003
	8000	11.4s	0.6997	0.4121	0.5384

Table 1: Dataset newsgroups1 results.

Experiments on 20 Newsgroups Data

We first study the clustering of different subsets of 20 newsgroups data collection. The collection consists of 18000 documents in 20 categories split into training and test subsets. We use four datasets with documents from randomly selected categories from

	t	time	AR	ARI	V-Meas.
FW	1000	0.37s	0.6587	0.5594	0.5929
	4000	1.38s	0.6674	0.5479	0.5866
	8000	2.6s	0.6679	0.5473	0.5864
PFW-B	1000	0.45s	0.7508	0.135	0.3555
	4000	1.57s	0.6172	0.6257	0.6364
	8000	2.06s	0.6172	0.6257	0.6364
PFW-V	1000	0.59s	0.6281	0.6095	0.6241
	4000	1.85s	0.6172	0.6257	0.6364
	8000	3.1s	0.6172	0.6257	0.6364
AFW-B	1000	0.41s	0.8653	0.0979	0.316
	4000	1.9s	0.6172	0.6257	0.6364
	8000	3.39s	0.6172	0.6257	0.6364
AFW-V	1000	0.48s	0.663	0.5548	0.5907
	4000	1.75s	0.6172	0.6257	0.6364
	8000	3.38s	0.6172	0.6257	0.6364
RD	1000	0.76s	1.0	0.0	0.0
	4000	4.67s	1.0	0.1795	0.333
	8000	13.52s	0.7585	0.4391	0.5161

Table 2: Dataset newsgroups2 results.

	t	time	AR	ARI	V-Meas.
FW	1000	0.41s	0.6756	0.5206	0.5879
	4000	1.35s	0.6468	0.5309	0.5975
	8000	2.63s	0.6473	0.5314	0.5978
PFW-B	1000	0.49s	0.758	0.217	0.4617
	4000	1.79s	0.6468	0.5317	0.6004
	8000	2.88s	0.6468	0.5317	0.6004
PFW-V	1000	0.56s	0.6468	0.5317	0.6004
	4000	1.96s	0.6468	0.5317	0.6004
	8000	3.71s	0.6468	0.5317	0.6004
AFW-B	1000	0.37s	0.8373	0.1381	0.3594
	4000	1.83s	0.6462	0.5316	0.6003
	8000	3.19s	0.6468	0.5317	0.6004
AFW-V	1000	0.49s	0.6468	0.5322	0.5993
	4000	1.63s	0.6468	0.5317	0.6004
	8000	2.99s	0.6468	0.5317	0.6004
RD	1000	0.86s	1.0	0.0	0.0
	4000	4.69s	0.9089	0.2212	0.3465
	8000	12.9s	0.8012	0.3526	0.4556

Table 3: Dataset newsgroups3 results.

the test subset. (i) *newsgroups1*: soc.religion.christian, comp.os.ms-windows.misc, talk.politics.guns, alt.atheism, talk.politics.misc. (ii) *newsgroups2*: comp.windows.x, sci.med, rec.autos, talk.religion.misc, sci.crypt. (iii) *newsgroups3*: misc.forsale, comp.sys.mac.hardware, talk.politics.mideast, sci.electronics, rec.motorcycles. (iv) *newsgroups4*: in comp.sys.ibm.pc.hardware, comp.graphics, rec.sport.hockey, rec.sport.baseball, sci.space. Each dataset has $k = 5$ true clusters and $1700 \leq n \leq 2000$ documents, where we use $K = 5$ for peeling off the computed clusters. We obtain the tf-idf (term-frequency times inverse document-frequency) vector for each document and then apply PCA to reduce the dimensionality to 20. We obtain the similarity matrix \mathbf{A} using the cosine similarity between the PCA vectors and then shift the off-diagonal elements by 1 to ensure nonnegative entries.

	t	time	AR	ARI	V-Meas.
FW	1000	0.42s	0.653	0.5097	0.5706
	4000	1.38s	0.6169	0.4672	0.5437
	8000	2.6s	0.7002	0.5014	0.5514
PFW-B	1000	0.43s	0.8092	0.2247	0.4483
	4000	1.82s	0.6697	0.6211	0.6484
	8000	3.04s	0.6697	0.6211	0.6484
PFW-V	1000	0.58s	0.6591	0.6446	0.6717
	4000	2.02s	0.6565	0.6462	0.675
	8000	2.74s	0.6565	0.6462	0.675
AFW-B	1000	0.35s	0.9041	0.1109	0.3361
	4000	1.87s	0.6687	0.6191	0.6463
	8000	3.55s	0.6697	0.6211	0.6484
AFW-V	1000	0.5s	0.6525	0.5071	0.5651
	4000	1.84s	0.6565	0.6462	0.675
	8000	3.6s	0.6565	0.6462	0.675
RD	1000	0.93s	1.0	0.0	0.0
	4000	5.46s	1.0	0.3197	0.4112
	8000	14.52s	0.8559	0.4528	0.5328

Table 4: Dataset newsgroups4 results.

Tables 1, 2, 3, and 4 show the results for the different datasets. We observe that different variants of FW yield significantly better results compared to replicator dynamics (RD), w.r.t. both ARI and V-Measure. In particular, PFW-V and AFW-V are computationally efficient and perform very well even with $t = 1000$. On the other hand, these methods are more robust w.r.t. different parameter settings. Since all the objects in the ground truth solutions are assigned to a cluster, the assignment rate (AR) indicates the ratio of the objects assigned (correctly or incorrectly) to a cluster during the clustering. High AR and low ARI/V-measure means assignment of many objects to wrong clusters. This is what happens for RD with $t = 1000$. We note that these results are consistent with the results on synthetic datasets reported in supplementary material.

As discussed in (Pavan and Pelillo 2007), it is common for DSC to perform a post processing to assign each unassigned object to the cluster which it has the highest average similarity with. Specifically, let $C_0 \subseteq V$ contain the unassigned objects and $C_i \subseteq V$, $1 \leq i \leq K$, be the predicted clusters. Object $j \in C_0$ is then assigned to cluster C_i that satisfies

$$i \in \arg \max_{\ell \geq 1} \frac{1}{|C_\ell|} \sum_{p \in C_\ell} \mathbf{A}_{jp}.$$

Table 5 shows the performance of different methods after assigning all the documents to valid clusters, i.e., when AR is always 1. We observe that ARI and V-measure are usually similar for pre and post assignment settings. In both cases the FW variants (especially PFW-V and AFW-V) yield the best and computationally the most efficient results. Consistent to the previous results, PFW-V and AFW-V yield high scores already with $t = 1000$.

Image Segmentation

Then, we study segmentation of colored images in HSV space. We define the feature vector $\mathbf{f}(i) =$

$[v, vs \sin(h), vs \cos(h)]^T$ as in (Pavan and Pelillo 2007), where h , s , and v are the HSV values of pixel i . The similarity matrix \mathbf{A} is then defined as follows. (i) Compute $\|\mathbf{f}(i) - \mathbf{f}(j)\|$, for every pair of pixels i and j to obtain \mathbf{D}^{L2} . (ii) Compute the minimax (path-based) distances (Fischer and Buhmann 2003; Chehreghani 2017; Haghiri Chehreghani 2017b) from \mathbf{D}^{L2} to obtain \mathbf{D}^P . (iii) Finally, $\mathbf{A} = \max(\mathbf{D}^P) - \mathbf{D}^P$, where \max is over the elements in \mathbf{D}^P as used in (Chehreghani 2016).

Figure 1 shows the segmentation results of the airplane image in Figure 1(a). The image has dimensions 120×80 , which leads to a clustering problem with $n = 120 \cdot 80 = 9600$. We run the FW variants for $t = 10000$ and RD for $t = 250$ iterations. Due to the linear versus quadratic per-iteration time complexity of the FW variants and RD, respectively, we are able to run FW for many more iterations. This allows us to have more flexibility in tuning the parameters and thus obtain more robust results. See (Johnell 2020) for additional details.

Conclusion

We presented a unified and computationally efficient framework to employ the different variants of Frank-Wolfe for Dominant Set Clustering. In particular, replicator dynamics was replaced with standard, pairwise, and away-steps Frank-Wolfe when optimizing the quadratic problem defined by DSC. We provided a specialized analysis of the algorithms' convergence rates, and demonstrated the effectiveness of the framework via several experimental studies.

Acknowledgment

The work of Morteza Haghiri Chehreghani was partially supported by the Wallenberg AI, Autonomous Systems and Software Program (WASP) funded by the Knut and Alice Wallenberg Foundation.

References

- [Bansal, Blum, and Chawla 2004] Bansal, N.; Blum, A.; and Chawla, S. 2004. Correlation clustering. volume 56, 89–113.
- [Bomze, Rinaldi, and Zeffiro 2019] Bomze, I. M.; Rinaldi, F.; and Zeffiro, D. 2019. Active set complexity of the away-step frank-wolfe algorithm. *arXiv preprint arXiv:1912.11492*.
- [Bühler and Hein 2009] Bühler, T., and Hein, M. 2009. Spectral clustering based on the graph p-laplacian. In *26th Annual International Conference on Machine Learning (ICML)*, 81–88.
- [Bulò and Pelillo 2017] Bulò, S. R., and Pelillo, M. 2017. Dominant-set clustering: A review. *European Journal of Operational Research* 262(1):1–13.
- [Bulò, Pelillo, and Bomze 2011] Bulò, S. R.; Pelillo, M.; and Bomze, I. M. 2011. Graph-based quadratic optimization: A fast evolutionary approach. *Computer Vision and Image Understanding* 115(7):984–995.

Method	t	newsgroups1		newsgroups2		newsgroups3		newsgroups4	
		ARI	V-Meas.	ARI	V-Meas.	ARI	V-Meas.	ARI	V-Meas.
FW	1000	0.4068	0.4969	0.5158	0.5733	0.5751	0.595	0.4663	0.5252
	4000	0.4639	0.5225	0.5084	0.5699	0.572	0.5962	0.4409	0.5084
	8000	0.4766	0.5351	0.5084	0.5699	0.5729	0.5972	0.4973	0.5396
PFW-B	1000	0.2063	0.3919	0.178	0.3814	0.2764	0.4859	0.288	0.4878
	4000	0.4623	0.5324	0.5332	0.5834	0.5734	0.5992	0.587	0.6094
	8000	0.4356	0.5219	0.5332	0.5834	0.5734	0.5992	0.587	0.6094
PFW-V	1000	0.5091	0.5763	0.5331	0.5824	0.5734	0.5992	0.605	0.6226
	4000	0.4298	0.5149	0.5332	0.5834	0.5734	0.5992	0.6072	0.6268
	8000	0.4356	0.5219	0.5332	0.5834	0.5734	0.5992	0.6072	0.6268
AFW-B	1000	0.0966	0.2751	0.131	0.344	0.1782	0.3967	0.1313	0.3577
	4000	0.3162	0.4806	0.5332	0.5834	0.5734	0.5992	0.588	0.6097
	8000	0.4615	0.5319	0.5332	0.5834	0.5734	0.5992	0.587	0.6094
AFW-V	1000	0.5066	0.5744	0.5099	0.5699	0.5741	0.5983	0.4592	0.5183
	4000	0.5047	0.5719	0.5332	0.5834	0.5734	0.5992	0.6072	0.6268
	8000	0.4308	0.5148	0.5332	0.5834	0.5734	0.5992	0.6072	0.6268
RD	1000	0.0	0.0	0.0	0.0	0.0	0.0	0.0	0.0
	4000	0.1892	0.3042	0.1795	0.333	0.2394	0.3575	0.3197	0.4112
	8000	0.3659	0.4937	0.4123	0.5065	0.4227	0.4973	0.4858	0.5556

Table 5: Result of different methods on 20 newsgroup datasets after post assignment of the unassigned documents.

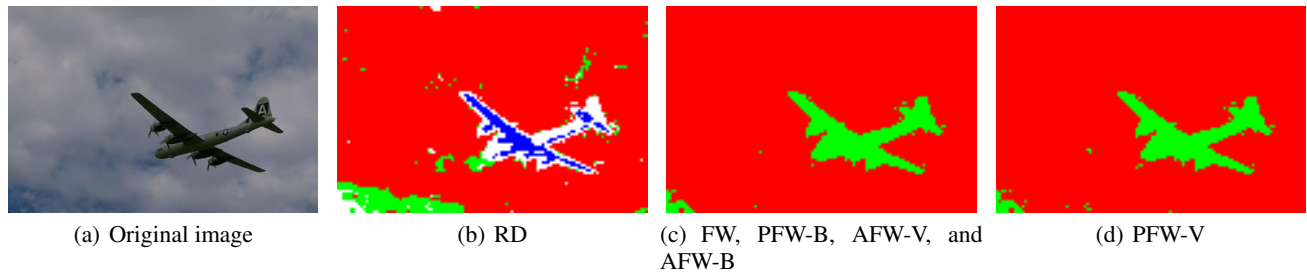


Figure 1: Original image and segmentation results.

- [Bulò, Torsello, and Pelillo 2009] Bulò, S. R.; Torsello, A.; and Pelillo, M. 2009. A game-theoretic approach to partial clique enumeration. *Image Vision Comput.* 27(7):911–922.
- [Chan, Schlag, and Zien 1994] Chan, P. K.; Schlag, M. D. F.; and Zien, J. Y. 1994. Spectral k-way ratio-cut partitioning and clustering. *IEEE Trans. on CAD of Integrated Circuits and Systems* 13(9):1088–1096.
- [Chehreghani 2016] Chehreghani, M. H. 2016. Adaptive trajectory analysis of replicator dynamics for data clustering. *Machine Learning* 104(2-3):271–289.
- [Chehreghani 2017] Chehreghani, M. H. 2017. Classification with minimax distance measures. In *Proceedings of the Thirty-First AAAI Conference on Artificial Intelligence*, 1784–1790. AAAI Press.
- [Fischer and Buhmann 2003] Fischer, B., and Buhmann, J. M. 2003. Path-based clustering for grouping of smooth curves and texture segmentation. *IEEE Transactions on Pattern Analysis and Machine Intelligence* 25(4):513–518.
- [Frank and Wolfe 1956] Frank, M., and Wolfe, P. 1956. An algorithm for quadratic programming. *Naval research logistics quarterly* 3(1-2):95–110.
- [Haghir Chehreghani et al. 2007] Haghir Chehreghani, M.; Rahgozar, M.; Lucas, C.; and Haghir Chehreghani, M. 2007. A heuristic algorithm for clustering rooted ordered trees. *Intell. Data Anal.* 11(4):355–376.
- [Haghir Chehreghani 2017a] Haghir Chehreghani, M. 2017a. Clustering by shift. In *IEEE International Conference on Data Mining, ICDM*, 793–798.
- [Haghir Chehreghani 2017b] Haghir Chehreghani, M. 2017b. Efficient computation of pairwise minimax distance measures. In *IEEE International Conference on Data Mining, ICDM*, 799–804.
- [Hein and Bühler 2010] Hein, M., and Bühler, T. 2010. An inverse power method for nonlinear eigenproblems with applications in 1-spectral clustering and sparse PCA. In *Advances in Neural Information Processing Systems (NIPS)*, 847–855.
- [Hubert and Arabie 1985] Hubert, L., and Arabie, P. 1985. Comparing partitions. *Journal of classification* 2(1):193–218.
- [Jain 2010] Jain, A. K. 2010. Data clustering: 50 years beyond k-means. *Pattern recognition letters* 31(8):651–666.
- [Johnell 2020] Johnell, C. 2020. Frank-Wolfe Optimization for Dominant Set Clustering. Master’s thesis, Chalmers Uni-

versity of Technology, Department of Computer Science and Engineering.

[Kulesza, Taskar, and others 2012] Kulesza, A.; Taskar, B.; et al. 2012. Determinantal point processes for machine learning. *Foundations and Trends® in Machine Learning* 5(2–3):123–286.

[Lacoste-Julien and Jaggi 2015] Lacoste-Julien, S., and Jaggi, M. 2015. On the global linear convergence of frank-wolfe optimization variants. In *Advances in Neural Information Processing Systems*, 496–504.

[Lacoste-Julien 2016] Lacoste-Julien, S. 2016. Convergence rate of frank-wolfe for non-convex objectives. *arXiv preprint arXiv:1607.00345*.

[Lin and Cohen 2010] Lin, F., and Cohen, W. W. 2010. Power iteration clustering. In *27th International Conference on Machine Learning (ICML)*, 655–662.

[Liu, Latecki, and Yan 2013] Liu, H.; Latecki, L. J.; and Yan, S. 2013. Fast detection of dense subgraphs with iterative shrinking and expansion. *IEEE Trans. Pattern Anal. Mach. Intell.* 35(9):2131–2142.

[Ng, Jordan, and Weiss 2001] Ng, A. Y.; Jordan, M. I.; and Weiss, Y. 2001. On spectral clustering: Analysis and an algorithm. In *Advances in Neural Information Processing Systems 14*, 849–856. MIT Press.

[Pavan and Pelillo 2003a] Pavan, M., and Pelillo, M. 2003a. Dominant sets and hierarchical clustering. In *Proceedings of the Ninth IEEE International Conference on Computer Vision*, volume 2, 362–. IEEE.

[Pavan and Pelillo 2003b] Pavan, M., and Pelillo, M. 2003b. A new graph-theoretic approach to clustering and segmentation. In *2003 IEEE Computer Society Conference on Computer Vision and Pattern Recognition, 2003. Proceedings.*, volume 1, I–I. IEEE.

[Pavan and Pelillo 2007] Pavan, M., and Pelillo, M. 2007. Dominant sets and pairwise clustering. *IEEE transactions on pattern analysis and machine intelligence* 29(1):167–172.

[Reddi et al. 2016] Reddi, S. J.; Sra, S.; Póczos, B.; and Smola, A. 2016. Stochastic frank-wolfe methods for non-convex optimization. In *2016 54th Annual Allerton Conference on Communication, Control, and Computing (Allerton)*, 1244–1251. IEEE.

[Rosenberg and Hirschberg 2007] Rosenberg, A., and Hirschberg, J. 2007. V-measure: A conditional entropy-based external cluster evaluation measure. In *Proceedings of the 2007 joint conference on empirical methods in natural language processing and computational natural language learning (EMNLP-CoNLL)*, 410–420.

[Shi and Malik 2000] Shi, J., and Malik, J. 2000. Normalized cuts and image segmentation. *IEEE Trans. Pattern Anal. Mach. Intell.* 22(8):888–905.

[Thiel, Haghir Chehreghani, and Dubhashi 2019] Thiel, E.; Haghir Chehreghani, M.; and Dubhashi, D. P. 2019. A non-convex optimization approach to correlation clustering. In *The Thirty-Third AAAI Conference on Artificial Intelligence*, 5159–5166.

Appendix A - Additional Experiments

In this section, we further investigate the proposed optimization framework for Dominant Set Clustering by performing additional experiments.

Experiments on Synthetic Data

For synthetic experiments, we fix $n = 200$ and $K = k = 5$, and assign the objects uniformly to one of the k clusters.

Let $\mu \sim \mathcal{U}(0, 1)$ be uniformly distributed and

$$\begin{cases} z = 0, & \text{with probability } p \\ z = 1, & \text{with probability } 1 - p, \end{cases}$$

where p is the noise ratio. The similarity matrix $\mathbf{A} = (a_{ij})$ is then constructed as follows:

$$\begin{cases} a_{ij} = a_{ji} = z\mu, & \text{if } i \text{ and } j \text{ are in the same cluster} \\ a_{ij} = 0, & \text{otherwise.} \end{cases}$$

For each parameter configuration, we generate a similarity matrix, perform the clustering five times and then report the average results in Figure 2. We observe that the different FW methods are considerably more robust w.r.t. the noise in pairwise measurements and yields higher quality results. Also, the performance of all FW variants is consistent with different parameter configurations, whereas RD is more sensitive to the number of iterations t and cutoff δ .

Multi-Start Dominant Set Clustering

Finally, as a side study, we study a combination of multi-start dominant set clustering with the peeling off strategy. For this, we perform the following procedure.

1. Sample a subset of objects, and use them to construct a number of starting points for the same similarity matrix.
2. Run an optimization method for each starting point.
3. Identify the nonoverlapping clusters from the solutions and remove (peel off) the corresponding objects from the similarity matrix.
4. Repeat until no objects are left or a sufficient number of clusters have been found.

This scenario can be potentially useful in particular when multiple processors can perform clustering in parallel. However, if all the different starting points converge to the same cluster, then there would be no computational benefit. Thus, here we investigate such a possibility for our optimization framework. For this, we consider the number of passes through the entire data, where a pass is defined as one complete run of the aforementioned steps. After the solutions from a pass are computed, they are sorted based on the function value $f(\mathbf{x})$. The sorted solutions are then permuted in a decreasing order, and if the support of the current solution overlaps more than 10% with the support of the other (previous) solutions, it is discarded. Each pass will therefore yield at least one new cluster. With K the maximum number of clusters to extract, there will be at most K passes. Thus in order for the method to be useful and effective, less than K passes should be performed.

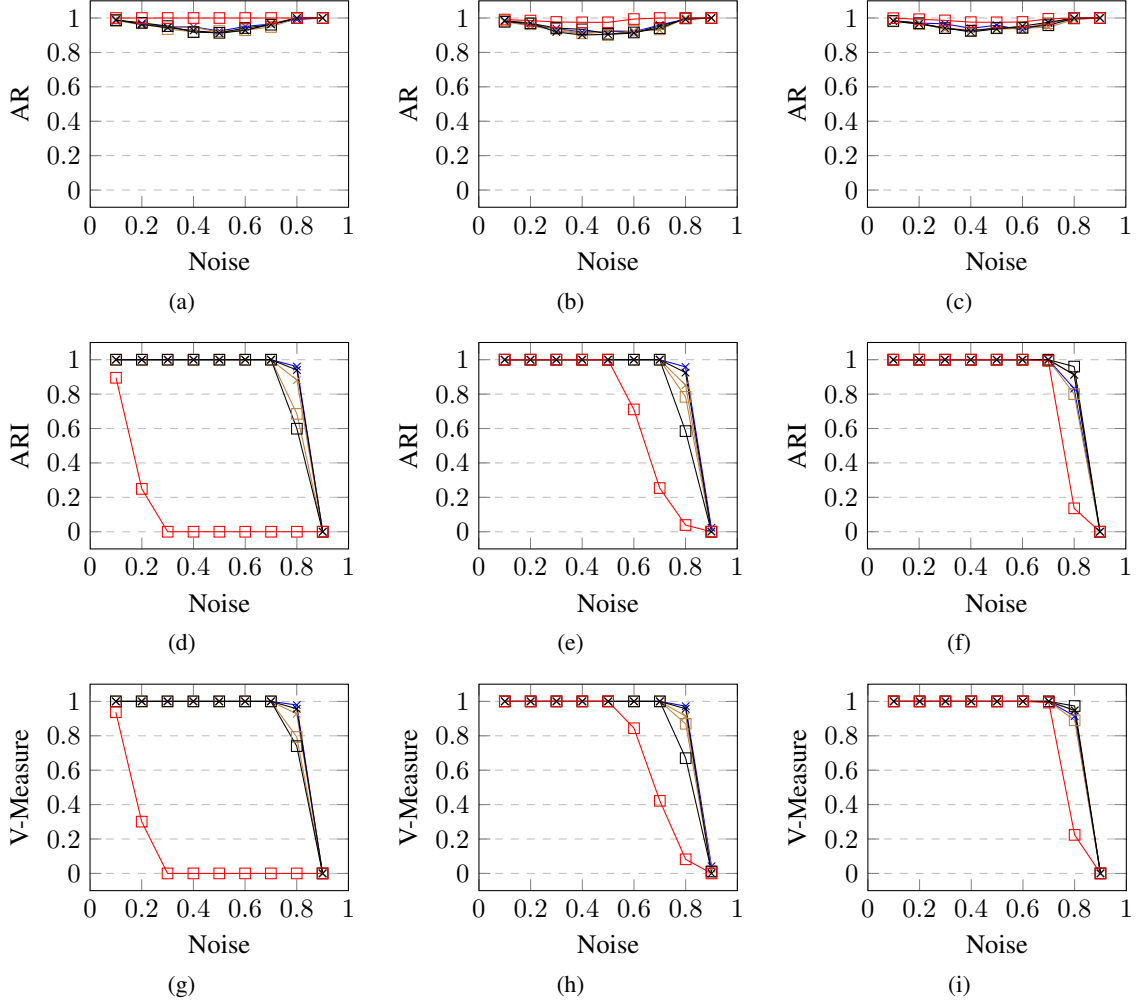


Figure 2: Results on the synthetic dataset for RD, FW, PFW, and AFW. PFW-B and AFW-B have squares; PFW-V and AFW-V have crosses. (a)-(i) $n = 200$. (a,d,g) $t = 400$, $\delta = 2 \cdot 10^{-12}$. (b,e,h) $t = 400$, $\delta = 2 \cdot 10^{-3}$. (c,f,i) $t = 4000$, $\delta = 2 \cdot 10^{-12}$.

Figure 3 shows the form of the datasets used in this study. Each cluster corresponds to a two dimensional Gaussian distribution with a fixed mean and an identity co-variance matrix (see Figure 3(a)). We fix $n = 1000$ and $K = k = 4$, and use the parameter p to control the noise ratio. Set $n_1 = pn$ and $n_2 = n - n_1$. A dataset is then generated by sampling n_1 objects from a uniform distribution (background noise in Figure 3(c)), $0.1 \cdot n_2$, $0.2 \cdot n_2$, $0.3 \cdot n_2$, and $0.4 \cdot n_2$ objects from the respective Gaussians.

Let \mathbf{D} be the matrix with pairwise Euclidean distances between all objects in the dataset. The similarity matrix is then defined as $\mathbf{A} = \max(\mathbf{D}) - \mathbf{D}$, similar to the image segmentation study but with a different base distance measure.

To determine the starting points we sample 4 components from $\{1, \dots, n\}$, denoted by i_1, i_2, i_3, i_4 . The number 4 matches the number of CPUs in our system. For a given component $i \in \{i_1, i_2, i_3, i_4\}$, we define the starting points as

$$\begin{cases} \bar{x}_i^V = 1 \\ \bar{x}_j^V = 0, & \text{for } j \neq i \end{cases}$$

and

$$\begin{cases} \bar{x}_i^B = 0.5 \\ \bar{x}_j^B = 0.5/(n-1), & \text{for } j \neq i. \end{cases}$$

FW uses only \bar{x}^V while PFW and AFW use both \bar{x}^V and \bar{x}^B .

To sample the components, we consider uniform sampling and Determinantal Point Processes (Kulesza, Taskar, and others 2012), denoted as UNI and DPP, respectively.

Uniform sampling. Let ℓ be the number of components to sample and $a_{i*} = \sum_{j=1}^n a_{ij}$, the sum of the elements in row i of \mathbf{A} . We sort a_{i*} 's in decreasing order, divide them into blocks of size n/ℓ , and sample one component i uniformly from each block.

Determinantal Point Processes (DPP). DPP is a common sampling method that provides both relevance and diversity. Thus, we study this method for sampling of starting objects too. A discrete DPP is a probability measure on subsets of a discrete set V , i.e., on the power set 2^V . We consider a variant of DPP called L -ensemble. If \mathbb{P}_L is an L -ensemble

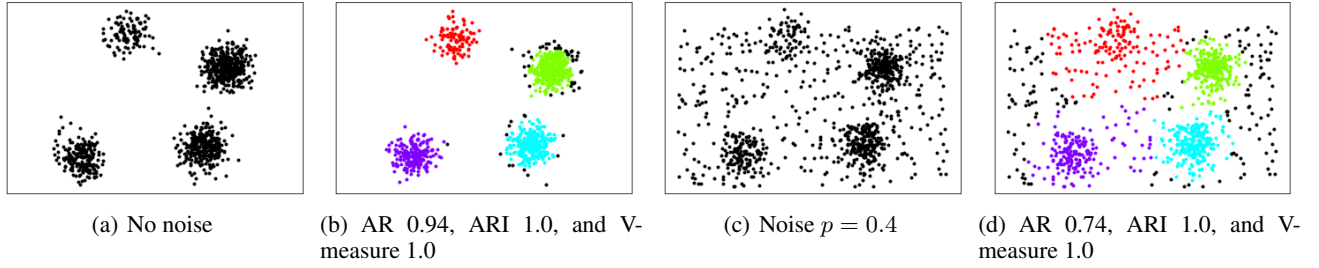


Figure 3: Two example datasets used for multi-start study. (b) and (d) show clustering results with the FW optimization; PFW and AFW produce similar results.

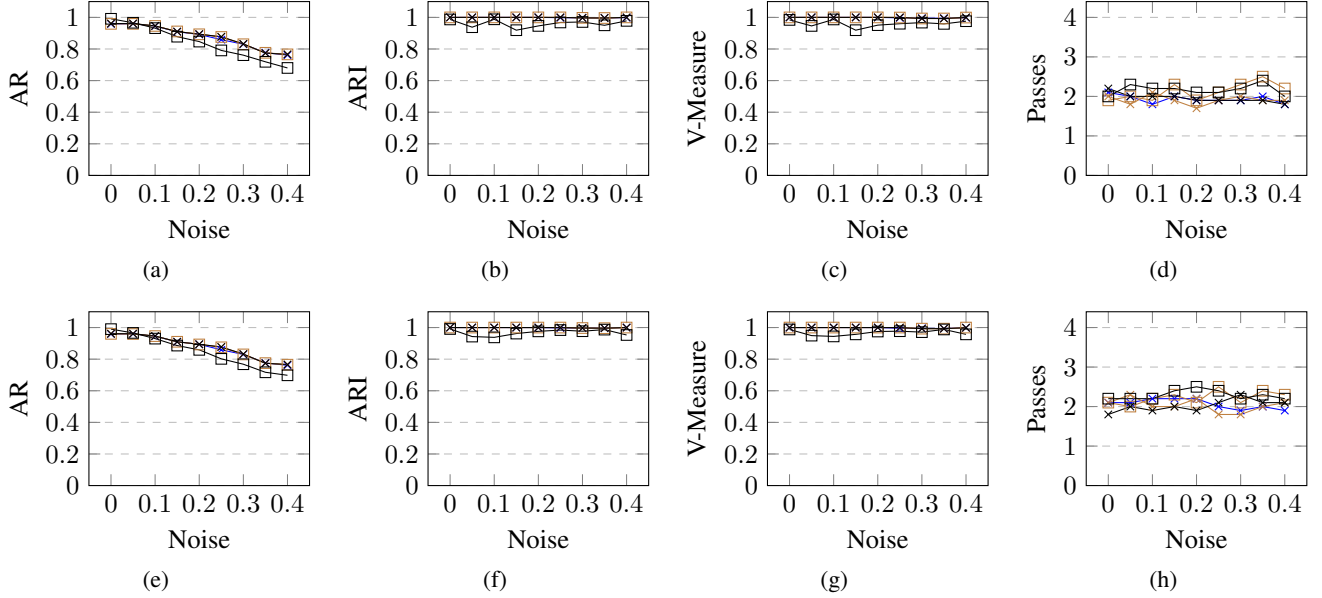


Figure 4: Results of multi-start paradigm with FW, PFW, and AFW where PFW-B and AFW-B are marked by squares; and PFW-V and AFW-V are marked by crosses. The first row corresponds to UNI and the second row corresponds to DPP sampling. All optimization and sampling methods require only about two passes to compute the clusters.

and $Y \subseteq V$, the probability of sampling it according to $\mathbb{P}_{\mathbf{L}}$ then is

$$\mathbb{P}_{\mathbf{L}}(Y) \propto \det(\mathbf{L}_Y),$$

where \mathbf{L} is real, symmetric, and positive semidefinite, called the likelihood matrix. The sub-matrix \mathbf{L}_Y is constructed of the rows and columns of \mathbf{L} indexed by Y (Kulesza, Taskar, and others 2012). If \mathbf{L} is a similarity matrix, then subsets with diverse objects (low similarities between them) are more likely to be sampled. For example, if $Y = \{i, j\}$, then

$$\mathbb{P}_{\mathbf{L}}(Y) \propto \det(\mathbf{L}_Y) = \ell_{ii}\ell_{jj} - \ell_{ij}\ell_{ji}. \quad (29)$$

Using the similarity matrix \mathbf{A} as the DPP likelihood matrix, we are more likely to sample objects that are diverse, and therefore less likely to belong in the same cluster.

The similarity matrix \mathbf{A} – or submatrices thereof – are real and symmetric, but not positive semidefinite since the main diagonal elements are zero. However, any symmetric matrix can be transformed to be positive semidefinite by ensuring it is diagonally dominant – every diagonal element is larger

than the sum of the absolute elements on the corresponding row.

In order to sample from a DPP with the given likelihood matrix, we need to compute its eigen-decomposition whose computational complexity can be $\mathcal{O}(n^3)$. Thus, we perform the sampling in two steps. The first step is similar to the uniform sampling method: we sort the components based on a_{i*} 's, split them into blocks of size $n/10$, and then uniformly sample $n^{2/3}/10$ objects from each block. In the second step we sample with DPP where for likelihood matrix we use the sub-matrix of \mathbf{A} indexed by the $n^{2/3}$ objects from the first step. Note that we ensure the sub-matrix of \mathbf{A} is diagonally dominant.

Results. Figure 4 illustrates the results for the different sampling methods and starting objects. For a given dataset, sampling method, and optimization method, we generate starting objects and run the experiments 10 times and report the average results. Each optimization method is run for $t = 1000$ iterations. For this type of dataset we do not observe any significant difference between FW, PFW, or AFW when using

either DPP or UNI. It seems that AFW with $\bar{\mathbf{x}}^B$ as starting object performs slightly worse.

However, we observe that all the sampling and optimization methods require only two passes, whereas we have $K = 4$. This observation implies that the multi-start paradigm is potentially useful for computing the clusters in parallel with the different FW variants.

Appendix B - Proofs

Proof of Lemma 1

Proof. By definition (lines 3 and 4 in Algorithm 2), $\mathbf{r}_0 = \mathbf{A}\mathbf{x}_0$ and $f_0 = \mathbf{x}_0^T \mathbf{A}\mathbf{x}_0$. Let $\mathbf{x} = \mathbf{x}_t$, $\mathbf{s} = \mathbf{s}_t$, and $\gamma = \gamma_t$. Assume $\mathbf{r}_t = \mathbf{A}\mathbf{x}$ and $f_t = \mathbf{x}^T \mathbf{A}\mathbf{x}$ holds. Expand the definition of $\mathbf{A}\mathbf{x}_{t+1}$ and proceed by induction.

$$\begin{aligned} \mathbf{A}\mathbf{x}_{t+1} &= \mathbf{A}((1 - \gamma)\mathbf{x} + \gamma\mathbf{s}) \\ &= (1 - \gamma)\mathbf{A}\mathbf{x} + \gamma\mathbf{A}\mathbf{s} \\ &= (1 - \gamma)\mathbf{r}_t + \gamma\mathbf{a}_{*i} \\ &= \mathbf{r}_{t+1}, \\ \mathbf{x}_{t+1}^T \mathbf{A}\mathbf{x}_{t+1} &= ((1 - \gamma)\mathbf{x} + \gamma\mathbf{s})^T \mathbf{A}((1 - \gamma)\mathbf{x} + \gamma\mathbf{s}) \\ &= (1 - \gamma)^2 \mathbf{x}^T \mathbf{A}\mathbf{x} + 2\gamma(1 - \gamma)\mathbf{s}^T \mathbf{A}\mathbf{x} + \gamma^2 \mathbf{s}^T \mathbf{A}\mathbf{s} \\ &= (1 - \gamma)^2 \mathbf{x}^T \mathbf{A}\mathbf{x} + 2\gamma(1 - \gamma)\mathbf{s}^T \mathbf{A}\mathbf{x} \\ &= (1 - \gamma)^2 f_t + 2\gamma(1 - \gamma)r_i^{(t)} \\ &= f_{t+1}. \end{aligned}$$

Note $\mathbf{s}^T \mathbf{A}\mathbf{s} = 0$ from the definition of \mathbf{s} and \mathbf{A} . \square

Proof of Lemma 2

Proof. Proceed as in proof of Lemma 1. Let $\mathbf{x} = \mathbf{x}_t$, $\mathbf{s} = \mathbf{s}_t$, $\mathbf{v} = \mathbf{v}_t$, and $\gamma = \gamma_t$.

$$\begin{aligned} \mathbf{A}\mathbf{x}_{t+1} &= \mathbf{A}(\mathbf{x} + \gamma(\mathbf{s} - \mathbf{v})) \\ &= \mathbf{A}\mathbf{x} + \gamma(\mathbf{A}\mathbf{s} - \mathbf{A}\mathbf{v}) \\ &= \mathbf{r}_t + \gamma(\mathbf{a}_{*i} - \mathbf{a}_{*j}) \\ &= \mathbf{r}_{t+1}, \\ \mathbf{x}_{t+1}^T \mathbf{A}\mathbf{x}_{t+1} &= (\mathbf{x} + \gamma(\mathbf{s} - \mathbf{v}))^T \mathbf{A}(\mathbf{x} + \gamma(\mathbf{s} - \mathbf{v})) \\ &= \mathbf{x}^T \mathbf{A}\mathbf{x} + 2\gamma(\mathbf{s} - \mathbf{v})^T \mathbf{A}\mathbf{x} \\ &\quad + \gamma^2(\mathbf{s} - \mathbf{v})^T \mathbf{A}(\mathbf{s} - \mathbf{v}) \\ &= \mathbf{x}^T \mathbf{A}\mathbf{x} + 2\gamma(\mathbf{s}^T \mathbf{A}\mathbf{x} - \mathbf{v}^T \mathbf{A}\mathbf{x}) - 2\gamma^2 a_{ij} \\ &= f_t + 2\gamma(r_i^{(t)} - r_j^{(t)}) - 2\gamma^2 a_{ij} \\ &= f_{t+1}. \end{aligned}$$

\square

Proof of Lemma 3

Proof. Proceed as in proof of Lemma 1. Let $\mathbf{x} = \mathbf{x}_t$, $\mathbf{v} = \mathbf{v}_t$, and $\gamma = \gamma_t$.

$$\begin{aligned} \mathbf{A}\mathbf{x}_{t+1} &= \mathbf{A}((1 + \gamma)\mathbf{x} - \gamma\mathbf{v}) \\ &= (1 + \gamma)\mathbf{A}\mathbf{x} - \gamma\mathbf{A}\mathbf{v} \\ &= (1 + \gamma)\mathbf{r}_t - \gamma\mathbf{a}_{*j} \\ &= \mathbf{r}_{t+1}, \\ \mathbf{x}_{t+1}^T \mathbf{A}\mathbf{x}_{t+1} &= ((1 + \gamma)\mathbf{x} - \gamma\mathbf{v})^T \mathbf{A}((1 + \gamma)\mathbf{x} - \gamma\mathbf{v}) \\ &= (1 + \gamma)^2 \mathbf{x}^T \mathbf{A}\mathbf{x} \\ &\quad - 2\gamma(1 + \gamma)\mathbf{v}^T \mathbf{A}\mathbf{x} + \gamma^2 \mathbf{v}^T \mathbf{A}\mathbf{v} \\ &= (1 + \gamma)^2 \mathbf{x}^T \mathbf{A}\mathbf{x} - 2\gamma(1 + \gamma)\mathbf{v}^T \mathbf{A}\mathbf{x} \\ &= (1 + \gamma)^2 f_t - 2\gamma(1 + \gamma)r_j^{(t)} \\ &= f_{t+1}. \end{aligned}$$

\square

Proof of Lemma 5

Proof. Let $\mathbf{y} = \mathbf{x}_t + \gamma_t \mathbf{d}_t$, for some ascent direction \mathbf{d}_t , $\mathbf{r}(\mathbf{x}) = \mathbf{A}\mathbf{x}$, and $f(\mathbf{x}) = \mathbf{x}^T \mathbf{A}\mathbf{x}$. From (15) we have

$$f(\mathbf{y}) = f(\mathbf{x}_t) + 2\gamma_t \mathbf{r}(\mathbf{x}_t)^T \mathbf{d}_t + \gamma_t^2 \mathbf{d}_t^T \mathbf{A} \mathbf{d}_t.$$

Using

$$\gamma_t = -\frac{(\mathbf{x}_t)^T \mathbf{A} \mathbf{d}_t}{\mathbf{d}_t^T \mathbf{A} \mathbf{d}_t} = -\frac{\mathbf{r}(\mathbf{x}_t)^T \mathbf{d}_t}{\mathbf{d}_t^T \mathbf{A} \mathbf{d}_t}$$

from (20), we get

$$\begin{aligned} f(\mathbf{y}) &= f(\mathbf{x}_t) - 2\frac{(\mathbf{r}(\mathbf{x}_t)^T \mathbf{d}_t)^2}{\mathbf{d}_t^T \mathbf{A} \mathbf{d}_t} + \frac{(\mathbf{r}(\mathbf{x}_t)^T \mathbf{d}_t)^2}{\mathbf{d}_t^T \mathbf{A} \mathbf{d}_t} \\ &= f(\mathbf{x}_t) - \frac{(\mathbf{r}(\mathbf{x}_t)^T \mathbf{d}_t)^2}{\mathbf{d}_t^T \mathbf{A} \mathbf{d}_t} \\ &\iff \\ (\mathbf{r}(\mathbf{x}_t)^T \mathbf{d}_t)^2 &= -\mathbf{d}_t^T \mathbf{A} \mathbf{d}_t (f(\mathbf{y}) - f(\mathbf{x}_t)). \end{aligned} \tag{30}$$

Let \mathbf{s}_t satisfy (13) and \mathbf{v}_t satisfy (14). Denote their nonzero components by i and j , respectively. Let $h_t = f(\mathbf{x}_{t+1}) - f(\mathbf{x}_t)$ and $g_t = 2(r(\mathbf{x}_t)_i - f(\mathbf{x}_t))$.

We consider the FW, away, and pairwise directions \mathbf{d}_t and corresponding step sizes satisfying $\gamma_t < \gamma_{max}$. Note that $f(\mathbf{y}) = f(\mathbf{x}_{t+1})$ holds in (30) for such directions and step sizes.

FW direction: Substitute $\mathbf{d}_t = \mathbf{s}_t - \mathbf{x}_t$ and (16) into (30).

$$\begin{aligned} (r(\mathbf{x}_t)_i - f(\mathbf{x}_t))^2 &= (2r(\mathbf{x}_t)_i - f(\mathbf{x}_t))h_t \\ \implies g_t^2 &\leq 4(2\bar{M} - \underline{M})h_t. \end{aligned}$$

Away direction: For this direction with $\gamma_t < \gamma_{max}$ we have

$$r(\mathbf{x}_t)_i - f(\mathbf{x}_t) < f(\mathbf{x}_t) - r(\mathbf{x}_t)_j,$$

from line 11 in Algorithm 4. Substitute $\mathbf{d}_t = \mathbf{x}_t - \mathbf{v}_t$ and (18) into (30).

$$\begin{aligned} (f(\mathbf{x}_t) - r(\mathbf{x}_t)_j)^2 &= (2r(\mathbf{x}_t)_j - f(\mathbf{x}_t))h_t \\ \implies g_t^2 &\leq 4(2\bar{M} - \underline{M})h_t. \end{aligned}$$

Pairwise direction: Substitute $\mathbf{d}_t = \mathbf{s}_t - \mathbf{v}_t$ and (17) into (30).

$$\begin{aligned} (r(\mathbf{x}_t)_i - r(\mathbf{x}_t)_j)^2 &= 2a_{ij}h_t \\ \implies g_t^2 &\leq 8\bar{M}h_t. \end{aligned}$$

Using previously defined I and β in section Analysis of Convergence Rates, we get

$$\begin{aligned} 4\beta(f(\mathbf{x}_t) - f(\mathbf{x}_0)) &= 4\beta \sum_{\ell=0}^{t-1} h_\ell \geq 4\beta \sum_{\ell \in I} h_\ell \\ &\geq \sum_{\ell \in I} g_\ell^2 \geq |I| \tilde{g}_t^2 \\ \implies \tilde{g}_t^2 &\leq \frac{4\beta(f(\mathbf{x}_t) - f(\mathbf{x}_0))}{|I|} \\ \iff \tilde{g}_t &\leq 2\sqrt{\frac{\beta(f(\mathbf{x}_t) - f(\mathbf{x}_0))}{|I|}}, \end{aligned}$$

for either direction \mathbf{d}_t . \square

Proof of Theorem 6

Proof. Since standard FW only takes good steps we have $|I| = t$. The result follows from Lemma 5. \square

Proof of Theorem 7

Proof. When $\gamma_t = \gamma_{max}$ we either have $|\sigma_{t+1}| = |\sigma_t| - 1$ or $|\sigma_{t+1}| = |\sigma_t|$, called drop and swap step, respectively. We need to upper bound the number of these steps in order to get a lower bound for $|I|$.

The following reasoning is from the analysis of PFW with convex objective function in (Lacoste-Julien and Jaggi 2015).

Let n be the dimension of \mathbf{x}_t , $m = |\sigma_t|$, and $\mathbf{d}_t = \mathbf{s}_t - \mathbf{v}_t$. Since we are performing line search, we always have $f(\mathbf{x}_\ell) < f(\mathbf{x}_t)$ for all $\ell < t$ that are nonstationary. This means the sequence $\mathbf{x}_0, \dots, \mathbf{x}_t$ will not have any duplicates. The set of component values does not change when we perform a swap step:

$$\{x_\ell^{(t)} : \ell = 1, \dots, n\} \cap \{x_\ell^{(t+1)} : \ell = 1, \dots, n\} = \emptyset.$$

That is, the components are simply permuted after a swap step. The number of possible unique permutations is $\kappa = n!/(n-m)!$. After we have performed κ swap steps, a drop step can be taken which will change the component values. Thus in the worst case, κ swap steps followed by a drop step will be performed until $m = 1$ before a good step is taken. The number of swap/drop steps between two good steps is then bounded by

$$\sum_{\ell=1}^m \frac{n!}{(n-\ell)!} \leq n! \sum_{\ell=0}^{\infty} \frac{1}{\ell!} = n!e \leq 3n!.$$

Result (26) follows from Lemma 5 and

$$|I| \geq \frac{t}{3n!}. \quad \square$$

Proof of Theorem 8

Proof. When $\gamma_t = \gamma_{max}$, \mathbf{d}_t must be the away direction. In this case the support is reduced by one, i.e. $|\sigma_{t+1}| = |\sigma_t| - 1$. Denote these indexes by D . Let $I_A \subseteq I$ be the indexes that adds to the support, i.e. $|\sigma_{t+1}| > |\sigma_t|$ for $t \in I_A$. Similar as before, we need to upper bound $|D|$ in order to get a lower bound for $|I|$.

We have $|I_A| + |D| \leq t$ and $|\sigma_t| = |\sigma_0| + |I_A| - |D|$. Combining the inequalities we get

$$\begin{aligned} 1 \leq |\sigma_t| &\leq |\sigma_0| + t - 2|D| \\ \implies |D| &\leq \frac{|\sigma_0| - 1 + t}{2}. \end{aligned}$$

Result (27) then follows from Lemma 5 and

$$|I| = t - |D| \geq t - \frac{(|\sigma_0| - 1 + t)}{2} = \frac{t + 1 - |\sigma_0|}{2}.$$

\square